HHS Public Access

Author manuscript

J Comput Assist Tomogr. Author manuscript; available in PMC 2020 January 01.

Published in final edited form as:

J Comput Assist Tomogr. 2019 ; 43(1): 143–148. doi:10.1097/RCT.0000000000000778.

Comparison of Navigator Triggering Reduced Field of View and Large Field of View Diffusion Weighted Imaging of the Pancreas

Lorenzo Mannelli, MD, PhD[1], **Serena Monti, PhD**[2], **Giuseppe Corrias, MD**[1,3], **Maggie M Fung, PhD**[4], **Charles Nyman**[1], **Jennifer S Golia Pernicka, MD**[1], and **Richard KG Do, MD, PhD**[1]

[1]Memorial Sloan-Kettering Cancer Center, Department of Radiology, New York, NY, United States

[2]IRCCS SDN, Naples, Italy

[3]University of Cagliari, Department of Radiology, via Università 40, Cagliari, Italy

[4]Global MR Applications and Workflow, GE Healthcare, New York, NY, United States

Structured Abstract

Rationale and objectives—The purpose of this study is to compare image quality, presence and grade of artifacts, signal-to-noise ratio (SNR), and apparent diffusion coefficient (ADC) values in pancreatic tissue between high resolution navigator triggered (NT) restricted field of view (rFOV) FOCUS single shot (SS) echo-planar imaging (EPI) diffusion weighted imaging (DWI) and NT large FOV SS-EPI DWI.

Materials and Methods—MRI examinations were performed with GE 3T systems using a 32-channel body array coil. Seventeen consecutive patients were imaged. A 5-point scale semi-quantitative grading system was utilized to evaluate image quality and general artifacts. SNR and ADC were measured in the head, body, and tail of the pancreas. Statistical analysis was performed using student t-test and Wilcoxon Signed Rank Test, with differences considered significant for $p<0.05$.

Results—More artifacts were present on large FOV compared to rFOV FOCUS SS-EPI DW images ($p < 0.01$). rFOV image quality was subjectively better ($p < 0.01$). No difference in the SNR was demonstrated between the two image datasets. ADC values were significantly lower ($p<0.01$) when calculated from rFOV images than large FOV images.

Conclusions—Our results demonstrate better image quality and reduced artifacts in rFOV images compared to large FOV DWI. Measurements from ADC maps derived from rFOV DWI

Corresponding author: Lorenzo Mannelli, M.D., Ph.D., Memorial Sloan-Kettering Cancer Center, Department of Radiology, Box 29, 1275 York Avenue, New York, NY 10065, Phone: 212 639-7293, Fax: 212 794-4010, mannellilorenzo@yahoo.it.

The authors disclose no conflict of interest.

Compliance with Ethical Standards

The authors have no conflict of interests to disclose.
This is a retrospective study involving human.
This article does not contain any studies with animals performed by any of the authors.
All procedures performed in studies involving human participants were in accordance with the ethical standards of the institutional and/or national research committee and with the 1964 Helsinki declaration and its later amendments or comparable ethical standards.
Informed consent was waived.

show significantly lower ADC values when compared to ADC maps derived from large FOV DWI.

Introduction

Diffusion-weighted imaging (DWI) initially found its applications in imaging of the brain in the 1980s and, in recent years, has become commonplace in body imaging to evaluate solid organs in both oncologic and non-oncologic populations (1). In particular, DWI is an evolving tool in evaluating pathologic conditions of the pancreas both qualitatively, by subjective evaluation of the images, and quantitatively, by measuring the apparent diffusion coefficient (ADC), a quantitative measure of water diffusivity (2). Diagnostic accuracy of various diseases, in particular pancreatic tumors, has improved through the use of high resolution DWI and is reported by Ichikawa et al. as a means to detect pancreatic adenocarcinoma with high sensitivity and specificity (1, 3).

Challenges to DWI of the pancreas remain, including its deep central location in the abdomen, far from the MRI coil elements (4, 5) and breathing motion. The susceptibility difference caused by metallic stents or surgical clips, or/and air in the adjacent stomach, transverse colon, and duodenum are a frequent source of image degradation resulting in both signal loss and spatial displacement of signal (4–7). Moreover, these inhomogeneity artifacts may alter ADC values.

Respiratory motion compensation is helpful in the acquisition of images of diagnostic quality and for visualizing fine anatomic details, as demonstrated in recent studies evaluating the image quality from respiratory-triggered, free-breathing, and breath-hold techniques for pancreatic adenocarcinoma (4, 8–15).

Recently, reduced Field of View (rFOV) FOCUS single shot diffusion weighted echo planar imaging (SS DW EPI) DWI has been introduced with the potential of higher resolution images in centrally located organs such as the prostate, spinal cord, and pancreas (4, 6, 16–18). Several studies have demonstrated superior image quality, reduced artifacts, and improved identification of small anatomic structures such as the pancreatic ducts when comparing rFOV imaging of the pancreas to conventional large FOV due to higher spatial resolution (3, 4, 8, 16, 17). In FOCUS a 2D spatially-selective echo-planar (in excitation k-space) radio-frequency excitation pulse reduces the excitation volume in both the phase encoding and slice select directions.

We hypothesized that a combination of rFOV FOCUS SS-EPI DWI with navigator echo respiratory triggering (NT) technique would allow for more robust and higher quality imaging compared to conventional large FOV SS-EPI DWI with NT.

The purpose of this study was to demonstrate the feasibility of high resolution NT focus rFOV FOCUS SS-EPI DWI in patients and to compare image quality, presence and grade of artifacts, signal-to-noise ratio (SNR), and apparent diffusion coefficient (ADC) values in pancreatic tissue between NT large FOV SS-EPI DWI and NT FOCUS rFOV SS-EPI DWI.

Materials and Methods

Patients

This retrospective study was approved by the local Institutional Review Board committee. Images of seventeen consecutive patients who underwent both large FOV and rFOV pancreas DWI with NT between August 2014 and January 2015 were reviewed. MR images were obtained from seventeen consecutive patients (6 males and 11 females, mean age 66.3 years, age range between 47 and 81 years) undergoing MRCP with both large FOV and rFOV DWI (Figure 1). The patients were referred for MRCP for: follow-up or initial evaluation of pancreatic cystic lesions (10 patients), staging/characterization of pancreatic solid mass (4 patients), elevated liver function tests (1 patient), pancreatic cancer screening in subject with family history of pancreatic cancer (1 patient), and intrahepatic cholangiocarcinoma (1 patient).

MRI technique

All MRI examinations were performed with GE 3T systems (MR750, GE Healthcare, USA) using a 32-channel body array receive coil. Small shim volume was placed at the pancreas location for more accurate shimming. Conventional large FOV SS-EPI DWI with ASPIR (Adiabatic SPectral Inversion Recovery) was acquired with the following parameters: FOV: 40 × 40 cm, matrix: 128 × 128, TE: 45.9ms, TI: 110ms, BW: 250 kHz, slice thickness: 8mm, number of slices 40, b-value 50 s/mm^2 (number of excitation pulses (NEX) = 1) and 500 s/mm^2 (NEX = 4), parallel imaging acceleration factor: 2, scan time: 1:24 min. rFOV FOCUS SS-EPI DWI was acquired with the following parameters: FOV: 24 × 12 cm, matrix: 160 × 80, TE: 46.6 ms, BW: 250 kHz, slice thickness: 6 mm, number of slices 15, b-value 50 s/mm^2 (NEX = 6) and 500 s/mm^2 (NEX = 16), scan time: 3:43 min. Navigator echo respiratory triggering technique was used for both large and rFOV DWI. The two sequences were acquired during the same session.

Image analysis

A semi-quantitative grading system was utilized to evaluate image quality and grade of artifacts. Presence of artifacts was assessed and, if present, subjectively rated for both large and rFOV DWI independently by two radiologists (with 9 and 10 years in abdominal MRI, respectively) with a five-point scale (1, no artifacts present; 2, minimal artifacts which do not interfere with diagnostic quality; 3, artifacts present which reduce diagnostic quality; 4, artifacts resulting in minimal diagnostic information; 5, non-diagnostic images). Image quality was subjectively rated by the same two radiologists with a five-point scale (1, optimal image quality; 2, image of diagnostic image quality; 3, image of limited diagnostic value/quality; 4, only minimal diagnostic content in the images; 5, non-diagnostic images).

Overall image quality for both large and rFOV DWI was also subjectively rated by two radiologists in consensus on a five point scale (1, optimal image quality; 2, image of diagnostic image quality; 3, image of limited diagnostic value/quality; 4, only minimal diagnostic content in the images; 5, non-diagnostic images).

Signal to noise ratio (SNR) and ADC were measured in the head, body, and tail of the pancreas on a dedicated workstation (GE Readyview, GE Healthcare, USA). rFOV images do not include areas outside of the body, thus air could not be used for SNR calculation. SNR was calculated as the ratio between the average signal intensity and the standard deviation of the signal intensity within a 0.5 cm diameter manually placed circular ROIs at the head, body and tail of the pancreas on the b500 images over the tissue of interest taking care to avoid areas with artifacts, intra-parenchymal vessels, and pancreatic duct. ADC maps were calculated in a monoexponential fashion on a pixel-by-pixel basis to form ADC maps, with the gray scale of the pixel linearly corresponding to the ADC values. Mean ADC values (mm^2/s) both at rFOV DWI and large FOV DWI were measured on ADC maps by manually placing 0.5 cm diameter circular ROIs at the head, body and tail of the pancreas on the b50 DW images over the tissue of interest taking care to avoid areas with artifacts, intra-parenchymal vessels, and pancreatic duct and copying and pasting the ROIs onto the ADC maps. ROIs were placed by a radiologist with 12 years of experience in abdominal MRI.

Statistical analysis

Statistical analysis comparing the ADC and SNR values was performed using student t-test with differences considered significant for $p < 0.05$. Wilcoxon Signed Rank Test was performed to compare the scores on image qualities and artifacts, with differences considered significant for two-tailed $p < 0.05$. Interreader agreement on image quality and artifacts was assessed by calculating the interclass correlation coefficient.

Results

Qualitative Analysis

Conventional large FOV and rFOV pancreas DWI with NT was feasible in all the subjects. Most of these patients were referred for follow up of pancreatic cystic lesions (11) while other reasons were evaluation of pancreatic solid masses (4), cholangiocarcinoma (1), and a family history of pancreatic cancer (1).

Presence of signal loss or ghosting artifacts within the pancreatic parenchyma was detected in 10 subjects, these were due to: air in the colon (3 subjects), air in the stomach (3 subjects) (figure 2), motion (1 subject), surgical clips (1 subject), surgical clips and air in the colon (1 subject), and motion and air in the colon (1 subject). Average artifact score was higher (3.06 ± 0.97) for large FOV compared to rFOV DW images (1.94 ± 0.75) (figure 1), with a statistically significant difference between the two image datasets ($p = 0.002$). The two readers incidentally noted fewer and less severe susceptibility-induced artifacts with the rFOV sequence.

Overall image quality was subjectively higher for the rFOV with NT images (figure 2) with an average score of 1.94 ± 0.90 for rFOV and 3.00 ± 1.01 for conventional large FOV ($p = 0.009$).

Interreader agreement on image quality and artifacts was excellent $k = 0.89$ and $k = 0.91$, respectively. The consensus reading was not used for statistical analysis but was deemed

necessary to eventually address discrepancies, because of the excellent agreement this was not needed.

Quantitative Analysis

Average SNR and ADC values are reported in tables I and II. There was no significant difference in the SNR between the two image datasets (figure 1) (all $p > 0.05$, see table I) although the SNR was higher in the head and body compared to the tail in rFOV DWI.

The ADC values in the head, body, and tail of the pancreas were significantly lower when calculated from rFOV images compared to large FOV images (Table II).

Discussion

In our experience combining rFOV pancreas FOCUS SS-EPI DWI with NT was feasible in all subjects and resulted in improved image quality and decreased artifacts compared to conventional large FOV SS-EPI DWI with NT. The average scan time for rFOV pancreas FOCUS SS-EPI DWI with NT was 3 minutes and 43 seconds.

DW MR imaging has been used to characterize different pancreatic pathologic entities, such as cystic lesions (19), neuroendocrine tumors (20), pancreatits and pancreatic adenocarcinoma (21). All of these studies have used qualitative assesment of images and DWI has been proved to rise radiologist confidence in diagnosing these entities. Furthermore ADC values allow a quantitive assement of different pathological processes and there are promising results that allow to differetiate these processes based on their mean ADC values. For example, it has been described how chronic pancreatitis has lower ADC compared to normal pancreas, which may be explained by fibrosis and reduction of exocrine tissue (22, 23). There are also different reports showing high sensitivity of DWI in detecteding pancreatic adenocarcinoma (24, 25), even though the specificity of ADC values for pancreatic adenocarcinoma detection is low due to some overlaps with values found in mass forming pancreatits (26, 27). Neuroendocrine pancreatic tumors show high signal intensity with high *b*-value DWI, probably because of their high cellularity and have ADC values lower than those of pancreatic adenocarcinoma (20). Most of this literature agrees on how DWI can be useful for increasing confidence in visual detection of solid pancreatic tumors and how ADC measurements may help for differential diagnosis as a supplement to other imaging modalities. However, there is an agreement about many limitations of conventional DWI of the pancreas, so far addressed as low SNR, particulary on high *b*-values, and limited spacial resolution. Also motion artifacts have been addressed as potential cause of errors in ADC calculation(28).

In our clinical practice, patients being evaluated for pancreatic lesions undergo Magnetic Resonance Cholangiopancreatography (MRCP) protocol (29–31). The rationale for introducing a rFOV DWI focused on the pancreas is to provide higher spatial resolution in order to evaluate pancreatic solid and cystic lesions and to help delineate abnormalities in relation to the pancreatic duct. The higher spatial resolution has the potential for enhancing our ability to detect subtle solid lesions, augmenting our ability to discriminate benign from malignant lesions, and/or providing an improved means of monitoring tumor response to

therapy. The rationale for introducing NT in rFOV DWI focused on the pancreas is to adress motion artifacts, improving ADC calculation.

Image quality scores were significantly higher in rFOV than in conventional large FOV DWI. The results of our study comparing artifacts and image quality are similar to those of another prior study (4), with one main difference: our study combines both rFOV with NT technique whereas others evaluated these two factors independently. The improved image quality and reduction of artifacts demonstrates the potential benefits of this technique in future standard of pancreatic DWI.

The readers incidentally noted fewer and less severe susceptibility-induced artifacts with the rFOV sequence, we speculate that this could be due to the reduced echo train length (ETL) in the rFOV sequence resulting in reduced distortion by susceptibility artifact. For FOCUS SS-EPI DWI a 2D spatially-selective echo-panar (in excitation k-space) RF excitation pulse reduces the excitation volume in both the phase encoding and slice select directions and the ETL is equal to the phase matrix, in our case 80. For traditional DWI, ETL is equal to the phase matrix divided by the parallel imaging acceleration factor; in our case 64 (128 diveded 2).

We demonstrated that rFOV with NT is feasible in our patient population with no differences in SNR in the pancreatic head, body, and tail even with higher in-plane spatial resolution (figure 3). This was achieved by increasing the number of excitations, with a 2–3 fold increase in acquisition time. The increase in spatial resolution has the potential to influence the differential diagnosis in clinical practice. For example, intraductal papillary mucinous neoplasm (IPMN) are more commonly multifocal compared to other cystic lesions of the pancreas; thus detection of additional lesions throughout the pancreas directs the differential diagnosis towards IPMN (figure 3) (29–33).

NT FOCUS rFOV SS-EPI has a smaller FOV and requires a longer acquisition time than NT large FOV SS-EPI DWI; these two sequences may either be integrated in the same protocol or if NT FOCUS rFOV SS-EPI is used to replace large FOV SS-EPI DWI, the user needs to be aware that several areas of the upper abdomen, such as portions of the liver, spleen, spine, and kidneys are not included in the field of view.

Lower ADC values for rFOV DWI compared to large FOV is of uncertain significance and is different from the findings of Ma et al. (4). While we do not have a clear explanation for this finding, we speculate that the reason for a difference in ADC values is possibly a reduction in artifacts on DW images that may affect ADC maps calculation as reported in other studies (6, 34). This has a potential clinical implication as prior large FOV DWI studies have shown mean ADCs of all pancreatic adenocarcinomas were significantly lower than that of the normal pancreatic tissues. Whether pancreatic adenocarcinoma would likewise demonstrate lower ADC values with rFOV DWI warrants further studies.

In our short series the pancreas was always included in the planned single rFOV. However, FOCUS rFOV allows for a limited number of slices to be acquired, thus the craniocaudal extension of the pancreas may represent a limitation to this imaging approach. This can be overcome by using two consecutive rFOVs; with the two rFOV including only the number of

slices need to cover the entire pancreas to keep the overall acquisition time within reasonable limits.

Our study has several limitations. First, the small sample size of patients undergoing both rFOV and large FOV with NT imaging was constrained by our retrospective study design, as rFOV DWI was available only on a fraction of our clinical scanners that underwent the requisite MRI scanner platform upgrades. Second, as noted above, we used more signal averages for the rFOV DWI to compensate for the smaller voxel size due to smaller slice thickness, which resulting in comparable SNR to large FOV DWI. A more direct comparison of rFOV to large FOV DWI would have entailed similar values for all acquisition parameters, and would have increased the SNR of the latter. However, we did not have a clinical justification to scan our patients with a large FOV with a greater number of signal averages. A comparison in volunteers could have avoided this limitation, but would potentially be less informative than our study performed in actual patients. Third, the subset of patients studied were primarily an oncologic, outpatient population because of our referral pattern. Our results may not be applicable to an inpatient population due to acute issues such as abdominal pain, and potential irregular breathing, which might reduce the feasibility of a rFOV DWI with NT sequence, possibly resulting in more artifacts and decreased subjective image quality. Fourth, all MR examinations were performed on the MR system of one particular vendor and; therefore, our results may not be readily transferable across MR systems from other vendors. Finally, a potential clinical limitation of rFOV is the inability to assess for lesions outside its FOV; a radiologist would have to assess the need to perform both rFOV and large FOV DWI sequences when evaluating patients undergoing MRCP, or always get both with the resulting time costs.

In conclusion, our preliminary results show that both rFOV and large DWI with NT can be obtained with similar SNR, but that rFOV DWI demonstrates improved overall image quality with reduced artifacts (Figure 4). We incidentally noted that in pancreatic DWI reduced echo train length results in reduced distortion by susceptibility artifact. Improved image quality is likely to increase sensitivity and specificity; however, we have not data to support this yet.

Acknowledgments

The authors Lorenzo Mannelli, Serena Monti, Giuseppe Corrias, Maggie Fung, Gregory Nyman, Jennifer Golia Pernicka, and Richard Do were equally involved in acquisition of data, analysis and interpretation of data, drafting of the manuscript, critical revision of the manuscript for important intellectual content, statistical analysis, technical, or material support of this study.

Grant support was provided by MSK Cancer Center Support Grant/Core Grant P30 CA008748

Work by Giuseppe Corrias was partially supported by a scholarship awarded by ISSNAF Imaging Science Chapter.

Abbreviations

ADC	apparent diffusion coefficent
BW	band widht
DWI	diffusion weighted imaging

EPI	echo-planar imaging
ETL	echo train length
FOCUS	reduced Field of View single shot diffusion weighted echo planar imaging diffusion weighted
FOV	field of view
GE®	General Electrics®
IPMN	intraductal papillary mucinous neoplasm
MRCP	magnetic resonance cholangiopancreatography
MRI	magnetic resonance imaging
NEX	number of excitations
NT	navigator triggered
RF	radio frequency
rFOV	restricted field of view
SNR	signal-to-noise ratio
SS	single-shot
TE	time to echo
TR	time to repetition

References

1. Ichikawa T, Haradome H, Hachiya J, Nitatori T, Araki T. Diffusion-weighted MR imaging with single-shot echo-planar imaging in the upper abdomen: preliminary clinical experience in 61 patients. Abdom Imaging. 1999; 24(5):456–61. [PubMed: 10475927]
2. Fukukura Y, Takumi K, Kamimura K, et al. Pancreatic adenocarcinoma: variability of diffusion-weighted MR imaging findings. Radiology. 2012; 263(3):732–40. DOI: 10.1148/radiol.12111222 [PubMed: 22623694]
3. Barral M, Taouli B, Guiu B, et al. Diffusion-weighted MR imaging of the pancreas: current status and recommendations. Radiology. 2015; 274(1):45–63. DOI: 10.1148/radiol.14130778 [PubMed: 25531479]
4. Ma C, Li YJ, Pan CS, et al. High resolution diffusion weighted magnetic resonance imaging of the pancreas using reduced field of view single-shot echo-planar imaging at 3 T. Magn Reson Imaging. 2014; 32(2):125–31. DOI: 10.1016/j.mri.2013.10.005 [PubMed: 24231348]
5. Koh DM, Collins DJ, Orton MR. Intravoxel incoherent motion in body diffusion-weighted MRI: reality and challenges. AJR Am J Roentgenol. 2011; 196(6):1351–61. DOI: 10.2214/AJR.10.5515 [PubMed: 21606299]
6. Korn N, Kurhanewicz J, Banerjee S, Starobinets O, Saritas E, Noworolski S. Reduced-FOV excitation decreases susceptibility artifact in diffusion-weighted MRI with endorectal coil for prostate cancer detection. Magn Reson Imaging. 2015; 33(1):56–62. DOI: 10.1016/j.mri.2014.08.040 [PubMed: 25200645]

7. Colagrande S, Belli G, Politi LS, Mannelli L, Pasquinelli F, Villari N. The influence of diffusion- and relaxation-related factors on signal intensity: an introductive guide to magnetic resonance diffusion-weighted imaging studies. J Comput Assist Tomogr. 2008; 32(3):463–74. DOI: 10.1097/RCT.0b013e31811ec6d4 [PubMed: 18520558]
8. Mannelli L, Nougaret S, Vargas HA, Do RK. Advances in diffusion-weighted imaging. Radiol Clin North Am. 2015; 53(3):569–81. DOI: 10.1016/j.rcl.2015.01.002 [PubMed: 25953290]
9. Legrand L, Duchatelle V, Molinie V, Boulay-Coletta I, Sibileau E, Zins M. Pancreatic adenocarcinoma: MRI conspicuity and pathologic correlations. Abdom Imaging. 2015; 40(1):85–94. DOI: 10.1007/s00261-014-0196-8 [PubMed: 25030776]
10. Lalwani N, Mannelli L, Ganeshan DM, et al. Uncommon pancreatic tumors and pseudotumors. Abdom Imaging. 2015; 40(1):167–80. DOI: 10.1007/s00261-014-0189-7 [PubMed: 25063236]
11. Kartalis N, Loizou L, Edsborg N, Segersvard R, Albiin N. Optimising diffusion-weighted MR imaging for demonstrating pancreatic cancer: a comparison of respiratory-triggered, free-breathing and breath-hold techniques. Eur Radiol. 2012; 22(10):2186–92. DOI: 10.1007/s00330-012-2469-3 [PubMed: 22549106]
12. Morita S, Ueno E, Suzuki K, et al. Navigator-triggered prospective acquisition correction (PACE) technique vs. conventional respiratory-triggered technique for free-breathing 3D MRCP: an initial prospective comparative study using healthy volunteers. J Magn Reson Imaging. 2008; 28(3):673–7. DOI: 10.1002/jmri.21485 [PubMed: 18777550]
13. Taouli B, Sandberg A, Stemmer A, et al. Diffusion-weighted imaging of the liver: comparison of navigator triggered and breathhold acquisitions. J Magn Reson Imaging. 2009; 30(3):561–8. DOI: 10.1002/jmri.21876 [PubMed: 19711402]
14. Zaharchuk G, Saritas EU, Andre JB, et al. Reduced field-of-view diffusion imaging of the human spinal cord: comparison with conventional single-shot echo-planar imaging. AJNR Am J Neuroradiol. 2011; 32(5):813–20. DOI: 10.3174/ajnr.A2418 [PubMed: 21454408]
15. Osman S, Lehnert BE, Elojeimy S, et al. A comprehensive review of the retroperitoneal anatomy, neoplasms, and pattern of disease spread. Curr Probl Diagn Radiol. 2013; 42(5):191–208. DOI: 10.1067/j.cpradiol.2013.02.001 [PubMed: 24070713]
16. Thierfelder KM, Sommer WH, Dietrich O, et al. Parallel-transmit-accelerated spatially-selective excitation MRI for reduced-FOV diffusion-weighted-imaging of the pancreas. Eur J Radiol. 2014; 83(10):1709–14. DOI: 10.1016/j.ejrad.2014.06.006 [PubMed: 25017152]
17. Riffel P, Michaely HJ, Morelli JN, et al. Zoomed EPI-DWI of the pancreas using two-dimensional spatially-selective radiofrequency excitation pulses. PLoS One. 2014; 9(3):e89468.doi: 10.1371/journal.pone.0089468 [PubMed: 24594702]
18. Thierfelder KM, Scherr MK, Notohamiprodjo M, et al. Diffusion-weighted MRI of the prostate: advantages of Zoomed EPI with parallel-transmit-accelerated 2D-selective excitation imaging. Eur Radiol. 2014; 24(12):3233–41. DOI: 10.1007/s00330-014-3347-y [PubMed: 25154727]
19. Inan N, Arslan A, Akansel G, Anik Y, Demirci A. Diffusion-weighted imaging in the differential diagnosis of cystic lesions of the pancreas. AJR Am J Roentgenol. 2008; 191(4):1115–21. DOI: 10.2214/AJR.07.3754 [PubMed: 18806153]
20. Bakir B, Salmaslioglu A, Poyanli A, Rozanes I, Acunas B. Diffusion weighted MR imaging of pancreatic islet cell tumors. Eur J Radiol. 2010; 74(1):214–20. DOI: 10.1016/j.ejrad.2009.02.003 [PubMed: 19264435]
21. Fattahi R, Balci NC, Perman WH, et al. Pancreatic diffusion-weighted imaging (DWI): comparison between mass-forming focal pancreatitis (FP), pancreatic cancer (PC), and normal pancreas. J Magn Reson Imaging. 2009; 29(2):350–6. DOI: 10.1002/jmri.21651 [PubMed: 19161187]
22. Sandrasegaran K, Akisik FM, Patel AA, et al. Diffusion-weighted imaging in characterization of cystic pancreatic lesions. Clin Radiol. 2011; 66(9):808–14. DOI: 10.1016/j.crad.2011.01.016 [PubMed: 21601184]
23. Sandrasegaran K, Nutakki K, Tahir B, Dhanabal A, Tann M, Cote GA. Use of diffusion-weighted MRI to differentiate chronic pancreatitis from pancreatic cancer. AJR Am J Roentgenol. 2013; 201(5):1002–8. DOI: 10.2214/AJR.12.10170 [PubMed: 24147470]

24. Kartalis N, Lindholm TL, Aspelin P, Permert J, Albiin N. Diffusion-weighted magnetic resonance imaging of pancreas tumours. Eur Radiol. 2009; 19(8):1981–90. DOI: 10.1007/s00330-009-1384-8 [PubMed: 19308414]
25. Takeuchi M, Matsuzaki K, Kubo H, Nishitani H. High-b-value diffusion-weighted magnetic resonance imaging of pancreatic cancer and mass-forming chronic pancreatitis: preliminary results. Acta Radiol. 2008; 49(4):383–6. DOI: 10.1080/02841850801895381 [PubMed: 18415779]
26. Muraoka N, Uematsu H, Kimura H, et al. Apparent diffusion coefficient in pancreatic cancer: characterization and histopathological correlations. J Magn Reson Imaging. 2008; 27(6):1302–8. DOI: 10.1002/jmri.21340 [PubMed: 18504750]
27. Lammer J, Herlinger H, Zalaudek G, Hofler H. Pseudotumorous pancreatitis. Gastrointest Radiol. 1985; 10(1):59–67. DOI: 10.1007/BF01893072 [PubMed: 2982692]
28. Ozaki M, Inoue Y, Miyati T, et al. Motion artifact reduction of diffusion-weighted MRI of the liver: use of velocity-compensated diffusion gradients combined with tetrahedral gradients. J Magn Reson Imaging. 2013; 37(1):172–8. DOI: 10.1002/jmri.23796 [PubMed: 22987784]
29. Buerke B, Domagk D, Heindel W, Wessling J. Diagnostic and radiological management of cystic pancreatic lesions: important features for radiologists. Clin Radiol. 2012; 67(8):727–37. DOI: 10.1016/j.crad.2012.02.008 [PubMed: 22520033]
30. Castelli F, Bosetti D, Negrelli R, et al. Multifocal branch-duct intraductal papillary mucinous neoplasms (IPMNs) of the pancreas: magnetic resonance (MR) imaging pattern and evolution over time. Radiol Med. 2013; 118(6):917–29. DOI: 10.1007/s11547-013-0945-8 [PubMed: 23801393]
31. Kang KM, Lee JM, Shin CI, et al. Added value of diffusion-weighted imaging to MR cholangiopancreatography with unenhanced mr imaging for predicting malignancy or invasiveness of intraductal papillary mucinous neoplasm of the pancreas. J Magn Reson Imaging. 2013; 38(3):555–63. DOI: 10.1002/jmri.24022 [PubMed: 23390008]
32. Nougaret S, Reinhold C, Chong J, et al. Incidental pancreatic cysts: natural history and diagnostic accuracy of a limited serial pancreatic cyst MRI protocol. Eur Radiol. 2014; 24(5):1020–9. DOI: 10.1007/s00330-014-3112-2 [PubMed: 24569848]
33. Song SJ, Lee JM, Kim YJ, et al. Differentiation of intraductal papillary mucinous neoplasms from other pancreatic cystic masses: comparison of multirow-detector CT and MR imaging using ROC analysis. J Magn Reson Imaging. 2007; 26(1):86–93. DOI: 10.1002/jmri.21001 [PubMed: 17659551]
34. Park JY, Shin HJ, Shin KC, et al. Comparison of readout segmented echo planar imaging (EPI) and EPI with reduced field-of-VIew diffusion-weighted imaging at 3t in patients with breast cancer. J Magn Reson Imaging. 2015; doi: 10.1002/jmri.24940

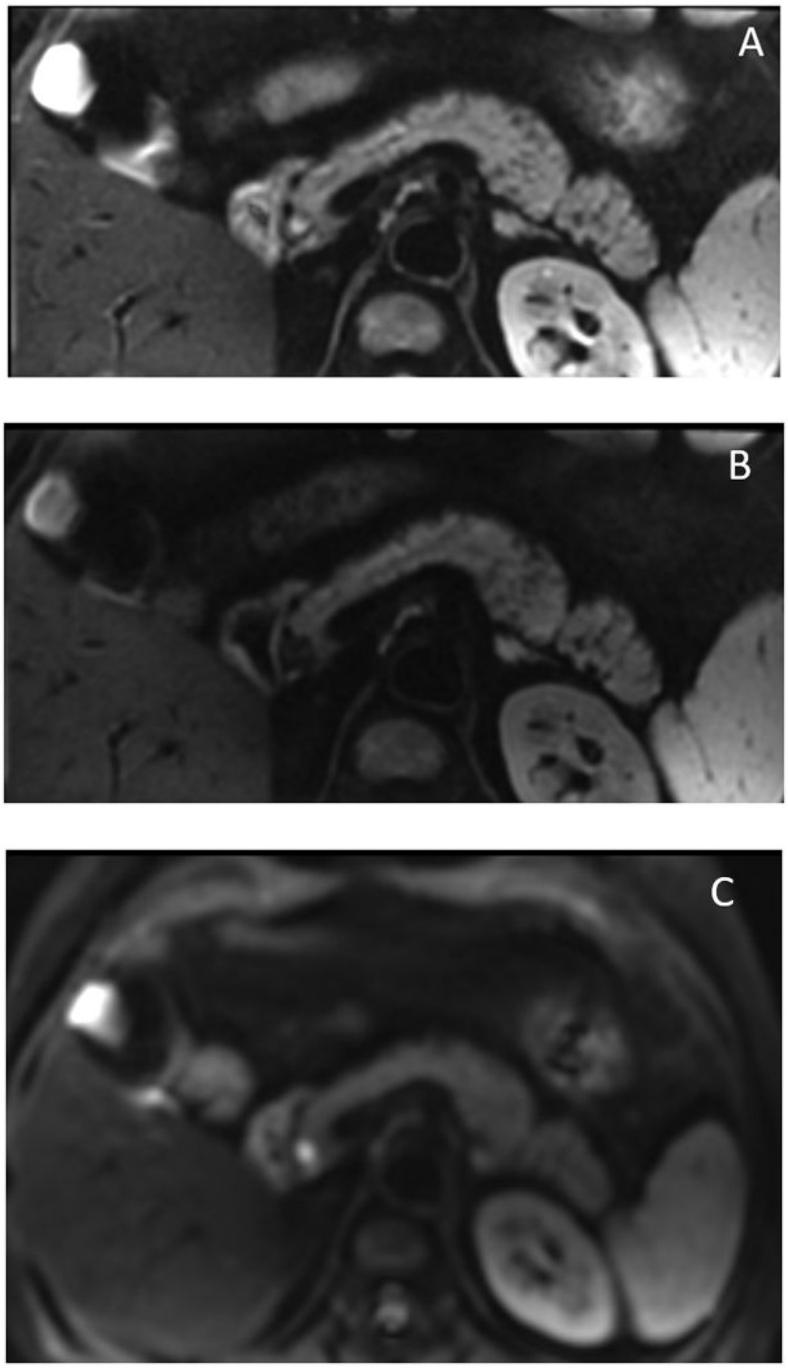

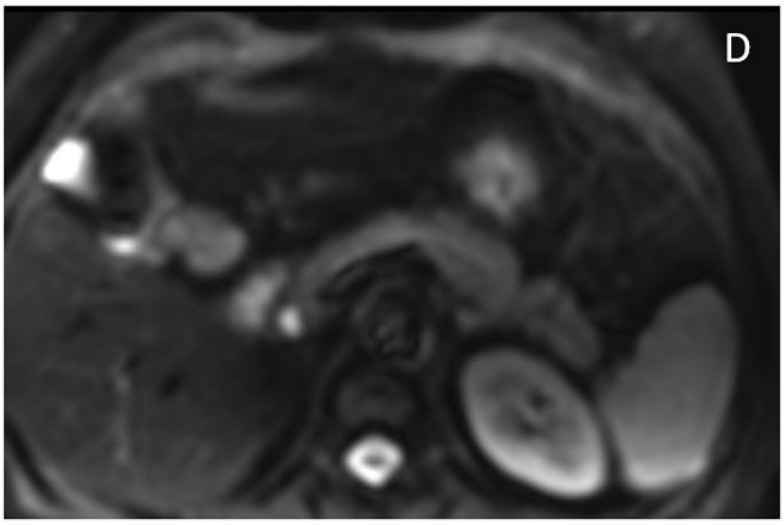

Figure 1.

b 50 NT ss DW EPI rFOV (A) and b 500 NT ss DW EPI rFOV (B) and b 50 large FOV (C) and b500 large FOV (D) images acquired at the same level in the same patient show no significant difference in mean SNR distribution. In rFOV image (A) resolution, number of signal averages, and acquisition time are increased compared to large FOV image (B). *DWI: diffusion weighted imaging; NT: not triggered; rFOV: restricted field of view; SS: single shot*

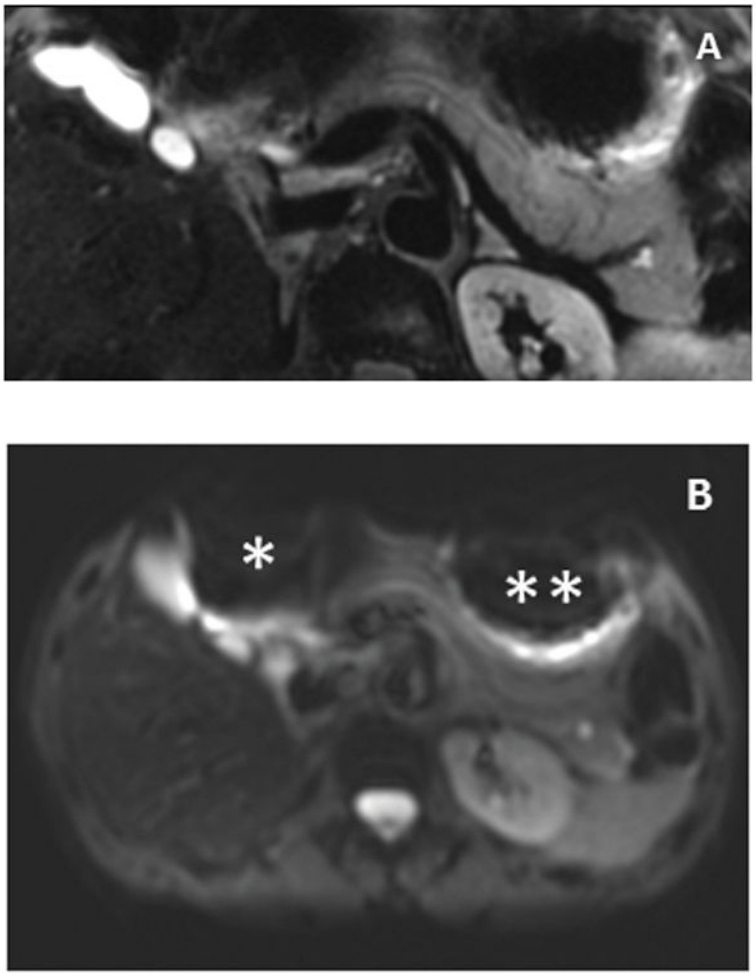

Figure 2.

b 50 NT ss DW EPI rFOV (A) and large FOV (B) images acquired at the same level in the same patient. In B evaluation of the pancreatic head and body is difficult due to susceptibility artifact caused by air in the transverse colon (white asterisk) and stomach (double asterisk). In rFOV DWI, the reduced echo train length results in reduced distortion by susceptibility artifact. *DWI: diffusion weighted imaging; NT: not triggered; rFOV: restricted field of view; SS: single shot*

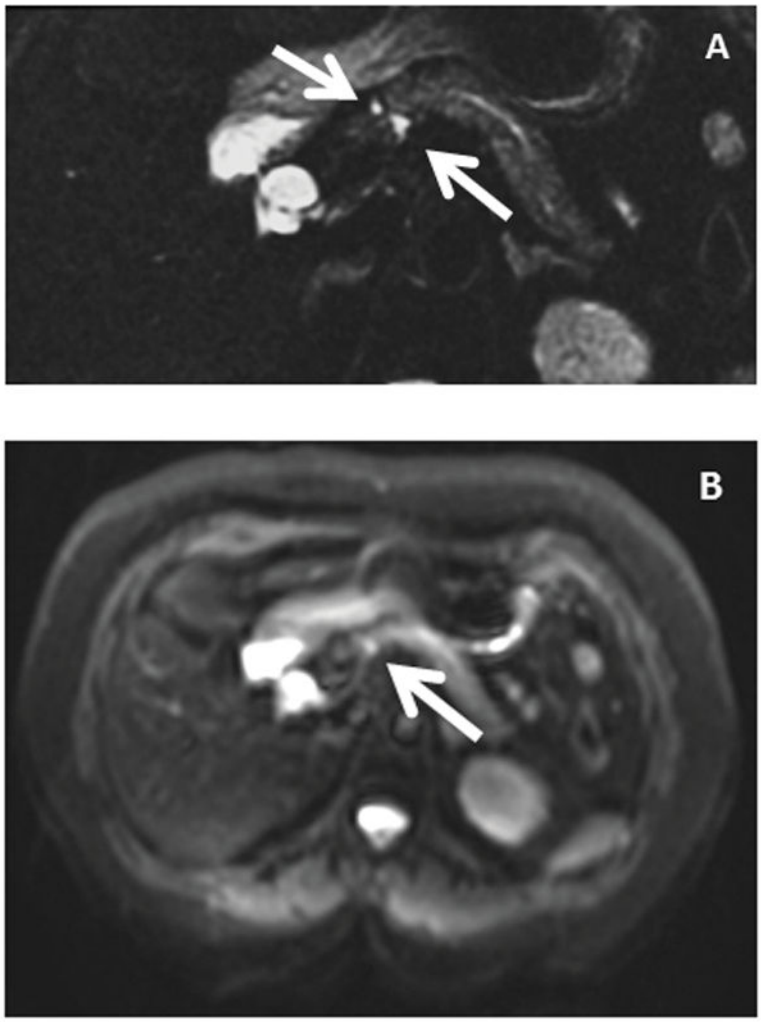

Figure 3.

b 50 NT ss DW EPI rFOV (A) and large FOV (B) images acquired at the same level in the same patient. Higher in-plane resolution allows identification of two small lesions in the pancreatic head (arrows in A), only one lesion (arrow in B) is visible in B. *DWI: diffusion weighted imaging; NT: not triggered; rFOV: restricted field of view; SS: single shot*

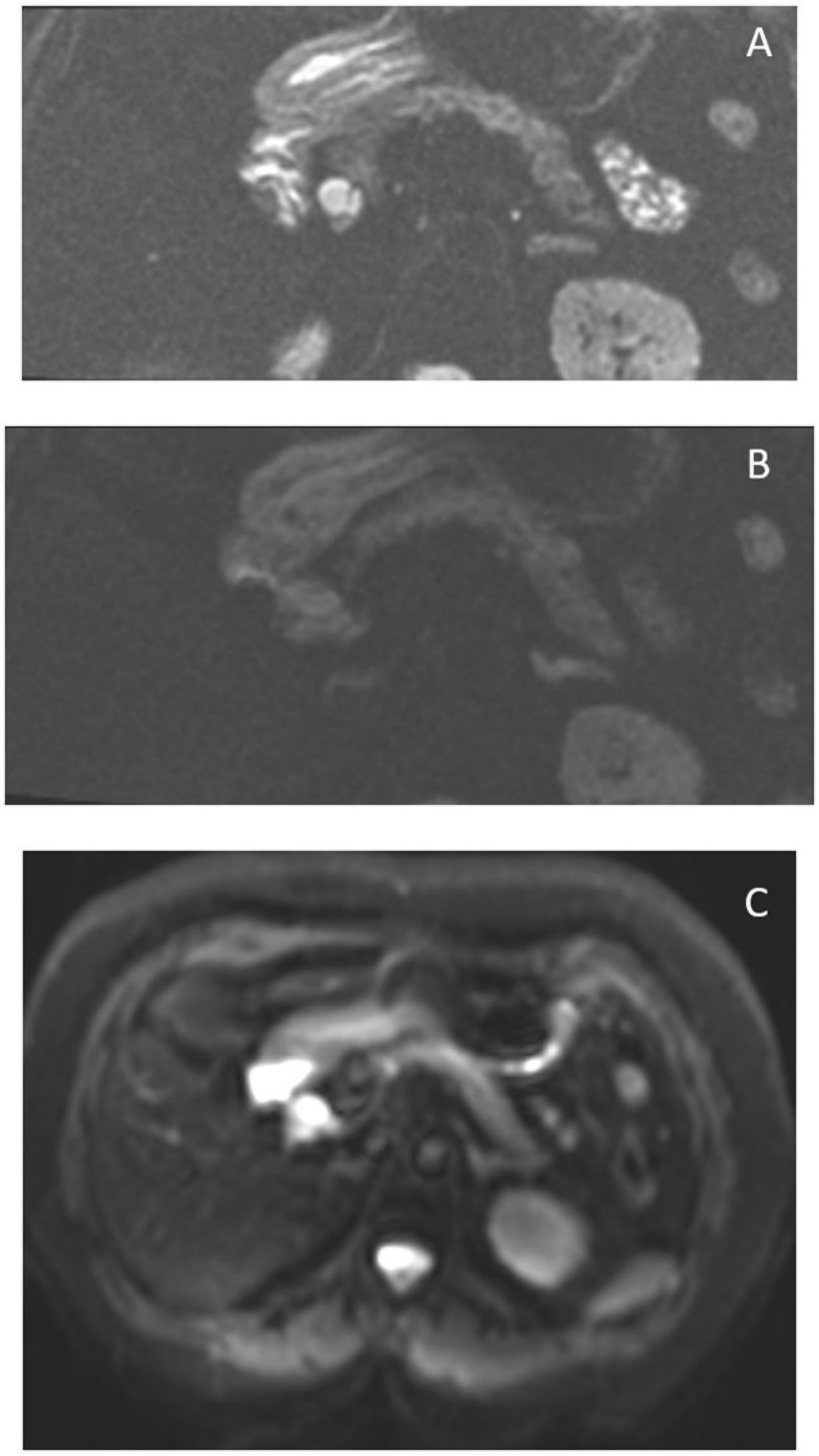

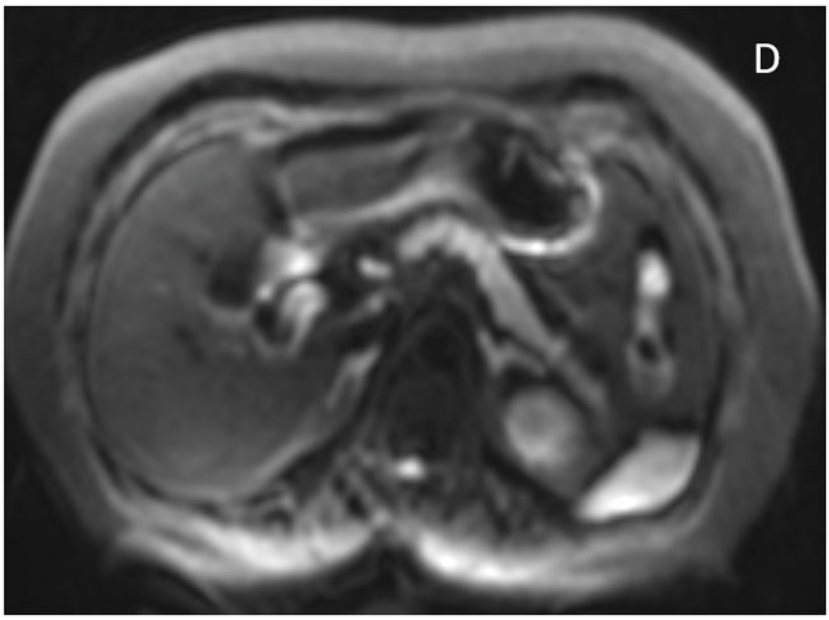

Figure 4.

b 50 NT ss DW EPI rFOV (A) and b 500 NT ss DW EPI rFOV (B) and b 50 large FOV (C) and b500 large FOV (D) images acquired at the same level in the same patient. In this particular case SNR was lower than for the rFOV images. In rFOV image (A) resolution, number of signal averages, and acquisition time are increased compared to large FOV image (B). *DWI: diffusion weighted imaging; NT: not triggered; rFOV: restricted field of view; SS: single shot*

Table I

	Large FOV	rFOV	student t-test
SNR head	9.00±4.3	10.20±2.3	0.23
SNR body	10.01±3.9	10.97±3.9	0.40
SNR tail	8.83±2.7	9.59±3.9	0.48

Signal-to-noise ration means ±standard deviation values of the b500 DWI for the head, body and tail of the pancreas for the large and restricted FOV. Student t test p values are reported in the third column.

Table II

	Large FOV×l0^{-3}mm^2/s	rFOV×10^{-3}rnm^2/s	student t-test
ADC head	2.20±0.5	1.75 ±0.3	0.022
ADC body	2.19±0.6	1.69±0.3	0.0007
ADC tail	2.23±0.5	1.90 ±0.4	0.005

ADC means ±standard deviation values (×10^{-3} mm^2/s) for the head, body and tail of the pancreas for the large and restricted FOV. Student t test p values are reported in the third column.